

# Results of XRF-Analyses and Thin Sections of Raw Materials from Beads

MELISSA GERLITZKI AND MANFRED MARTIN

## Introduction

This mineralogical and geochemical study presents the results of our analyses on 31 Neolithic beads which were found at the late Pre-Pottery Neolithic site of Ba`ja, southern Jordan (Tables 1-3, 5). 22 of them were discovered during the fieldwork for the *Household and Death Project* (2016-2021), hosted by the Institute for Near Eastern Archaeology at Free University of Berlin and co-directed by Hans Georg K. Gebel, Marion Benz, and Christoph Purschwitz.<sup>1</sup> The contexts are described in Alarashi this volume (Appendix 1), Benz *et al.* (this volume; Appendix 1), and Gebel *et al.* (2020). The remaining nine beads were uncovered in previous seasons between 1997-2007, during the excavations led by Hans Georg K. Gebel (for further references see Gebel *et al.* 2017).

With the increase in sedentary village life, stone beads of various minerals gained in importance during the early Holocene in the Levant, adding a new dimension of control to the panoply of ornaments in regard to colour and shape. During the Natufian shells, animal teeth, antler, egg-shells, bone beads, and pendants had dominated (for summaries with further references see Bar-Yosef 1991; Goring-Morris 1991; Maréchal 1991; Reese 1991; Hermansen 2004; Bar-Yosef Mayer and Porat 2008; Alarashi 2014; Baysal 2017; Kodaş 2019). Most of the analyses of raw materials focussed on the so-called “greenstone” beads and minerals (*e.g.*, Balzi *et al.* 1998; Hauptmann 2004; Maier 2008; Pfeiffer 2013;

*cf.* Santallier *et al.* 1997; Wright *et al.* 2008), possibly encouraged by the interest in copper technology and the huge amount of “greenstone” beads from Northern Mesopotamia (Hauptmann 2007). Unfortunately, raw data of bead analyses from Basta (Hauptmann 2004) and Beidha (Maier 2008) have not been published and are therefore not available for direct comparisons.

Besides “greenstones” and seashells, other exotic materials such as carnelian, coral, agate, and marble were exchanged too (Hermansen 2004, n.d.; Alarashi 2014, 2016). At Ba`ja, it seems that the colour contrast between shades of red and white played an important role (Hermansen this volume; Benz this volume; *cf.* Clarke 2012) with turquoise, chrysocolla, and amazonite beads having long object “biographies”. Often, they were used as rare contrasts to the dominant red-yellow-white patterns (Alarashi a this volume). Only in one instance, did we find a complete bracelet made almost exclusively of turquoise plus a few other “greenstones” and one limestone bead (Gebel *et al.* 2020; Benz *et al.* this volume).

In archaeology, the term “greenstone” is used for all green coloured mineral materials (Hauptmann 2004). In contrast the term “greenstone” in geoscience is applied to dark green, altered or metamorphosed igneous rocks. During fieldwork on the *Household and Death Project*, many ornament elements made of “greenstones” and of other minerals were found. Their raw material was identified in the field only preliminarily. Therefore, a representative sample of beads was exported to Germany in order to examine the raw material qualities (optical, physical, chemical as well as mineralogical contents) more precisely from a geoscientific perspective. The aim was to

<sup>1</sup> The beads were exported as two one-year loans with the permit numbers (12/5/274 and 1334). The analyses of the beads were financed by the German Research Foundation (BO 1599/16-1) and by a grant of the Franz-and-Eva-Rutzen-Foundation.

Table 1 Chemical composition of turquoise beads. Non-det.=not analysed, fields without numbers had a content below <0.005%.

Object	100814.W Box 3 ECXXX	100814.166	100814.117	100814.Zc	100814.Zb	60836	100809
Locus	C1:46	C1:46	C1:46	C1:46	C1:46	BNR27:100	DR25:101
SiO <sub>2</sub> [%]	28.31	11.10	18.48	11.57	26.95	32.95	13.44
Al <sub>2</sub> O <sub>3</sub> [%]	13.58	41.60	21.48	34.29	25.38	26.22	37.48
Fe <sub>2</sub> O <sub>3</sub> [%]	30.99	1.41	3.98	1.95	2.76	4.23	1.32
MgO [%]			2.96	0.694	0.799	1.23	0.946
CaO [%]	7.98	3.86	6.80	3.85	4.32	5.59	3.86
Na <sub>2</sub> O [%]			4.36	1.42	1.38	0.176	
K <sub>2</sub> O [%]	0.324	0.372	0.320	0.525		0.477	0.376
P <sub>2</sub> O <sub>5</sub> [%]	10.01	22.03	29.54	26.33	24.43	15.16	25.83
SO <sub>3</sub> [%]	0.471	0.362	0.339	0.306	0.398	0.422	0.444
Ba [%]						0.170	0.134
Cl [%]	0.231	0.284	0.686		0.418	0.157	0.072
Co [%]	0.029			0.318			0.013
Cu [%]	7.45	18.49	9.61	18.18	12.00	12.41	15.90
Cr [%]	0.057	0.144	0.366	0.209	0.193	0.050	0.026
Mn [%]	0.053		0.156		0.161	0.117	0.073
Mo [%]			0.043		0.021		
Ni [%]	0.140	0.128	0.319	0.173	0.265	0.054	0.016
Sr [%]	0.324	0.131	0.076	0.068	0.089	0.429	0.034
Ti [%]	0.056					0.158	0.040
Y [%]		0.102		0.100			
Zn [%]			0.497		0.413		
<b>Total</b>	<b>100.0</b>	<b>100.0</b>	<b>100.0</b>	<b>100.0</b>	<b>100.0</b>	<b>100.0</b>	<b>100.0</b>
Density [g/cm <sup>3</sup> ]	2.95	2.67	2.75	2.67	2.67	2.68	non-det.
Colour Texture	light blue to blue-green, dominant inter-growth with brown minerals (probably Fe)	light blue to blue-green, small inter-growth with brown minerals (probably Fe)	light blue to blue-green, small inter-growth with brown minerals (probably Fe)	light blue to blue-green, intergrowth with brown minerals (probably Fe)	light blue, small intergrowth with brown minerals (probably Fe)	light blue, inter-growth with brown minerals (probably Fe)	light blue, inter-growth with brown minerals (probably Fe)

get more information on provenance, on exchange networks and on whether there were spatial or chronological differences in the access to exotic goods at the Late to Final Pre-Pottery Neolithic B (Late PPNB/ Final PPNB) site of Ba`ja. The results show that local as well as distant raw materials were used for the manufacture of beads, and that a wide variety of greenstone sources were exploited, possibly including an until yet unidentified source of turquoise. However, for a precise determination of provenance, systematic investigations on trace elements and isotope analyses on ores and artefacts are indispensable.

## Material and Methods

As a first step all beads were described microscopically in terms of their colour and texture. A Zeiss microscope Stemi SV 11 was used for the analyses and a Canon EOS 600D camera for the photographic documentation. Then the beads were weighed, and their density was determined.

For thin section preparation, selected disk beads were mounted on a glass slide and then lapped to a thickness of about 27µm. Afterwards they were covered with a thin glass

Table 2 Chemical composition of chrysocolla and amazonite beads. Non-det.=not analysed, fields without numbers had a content below <0.005%.

Object	110825. 917	110825. 916	110825. 788A	110825. 788B	110825. 788C	110825. 787	110825. 854	0804.2	805	30800
Locus	CR28.2: 122a	CR28.2: 122a	CR28.2: 122a	CR28.2: 122a	CR28.2: 122a	CR28.2: 122a	CR28.2: 122a	C2:11	C12:20	F10:22
SiO <sub>2</sub> [%]	36.08	30.96	27.95	25.97	17.69	32.89	35.24	31.99	23.42	57.55
Al <sub>2</sub> O <sub>3</sub> [%]	6.49	5.36	3.82	6.00	4.81	4.35	6.24	4.31	4.69	16.43
Fe <sub>2</sub> O <sub>3</sub> [%]	0.323	3.90	4.80	5.23	12.96	1.18	0.49	0.31	1.67	2.01
MgO [%]	0.830	0.741	0.70	0.86	1.76	0.89	0.80	0.61	4.66	0.54
CaO [%]	1.90	2.80	2.31	5.66	6.99	1.93	1.80	2.14	6.14	3.24
Na <sub>2</sub> O [%]	0.339	0.221	0.220	0.259	0.312	0.235	0.203			1.323
K <sub>2</sub> O [%]	0.652	0.694	0.946	0.747	0.429	0.845	0.907	0.185	0.605	15.067
P <sub>2</sub> O <sub>5</sub> [%]	1.38	5.63	5.76	6.10	11.24	1.80	1.45	1.00	1.76	3.11
SO <sub>3</sub> [%]	0.187	0.297	0.281	0.302	0.484	0.144	0.206	0.071	0.190	0.079
Ba [%]									0.564	
Cl [%]	1.11	0.708	0.490	0.866	1.22	0.501	0.695	0.064	0.036	0.200
Co [%]									0.005	
Cu [%]	50.62	46.77	50.35	45.33	36.34	54.01	51.79	58.58	55.51	0.10
Cr [%]	0.033	1.55	1.81	2.12	4.59					0.123
F [%]									0.318	
Mn [%]	0.065	0.182	0.329	0.283	0.598	0.152	0.099	0.574	0.297	
Ni [%]		0.174	0.240	0.212	0.598				0.012	0.109
Pb [%]						0.904				
Sr [%]									0.044	
Ti [%]				0.069				0.030	0.086	0.121
V [%]						0.171				
Y [%]									0.006	
<b>Total</b>	<b>100.0</b>	<b>100.0</b>	<b>100.0</b>	<b>100.0</b>	<b>100.0</b>	<b>100.0</b>	<b>99.9</b>	<b>99.9</b>	<b>100.0</b>	<b>100.0</b>
Density [g/cm <sup>3</sup> ]	non-det.	non-det.	non-det.	non-det.	non-det.	non-det.	non-det.	non-det.	non-det.	2.56
Colour Texture	light green	light to dark green, recently broken	light to dark blue, recently broken	light to dark green	light to dark green, recently broken	light to dark green, recently broken	light blue, inter- growth	light green	light to dark green, compact	light blue/ green

slide. For analysis a *Zeiss* polarization microscope was used.

For the determination of the chemistry of the beads, X-ray fluorescence (XRF) spectroscopy was used. The XRF spectroscope utilised in this study is an *Axios Max* by *Malvern Panalytical* (former *PANalytical*). Usually, in geoscience

XRF analysis is performed with pulverised samples prepared as pressed powder tablets or fused discs. Here a non-destructive method of XRF had to be used. *Omnian* by *PANalytical*, is a programme for semi-quantitative analysis which allows one to perform a screening of nearly all elements occurring on the surface of the beads without destroying them.

The analyses were performed in the X-ray laboratory of the “State Authority for Geology, Mineral Resources and Mining” of Baden-Württemberg, Germany.

The 31 beads are classified into three groups. The first group describes the so-called “greenstone” beads in the archaeological sense of the word (Hauptmann 2004). Those beads are identified as turquoise or as chrysocolla beads based on their chemical composition. Amazonite has been grouped according to archaeological classification within this group, even though it is a Potassium-Aluminium-Silicate. The second group describes the limestone beads. In this group, predominantly marine and freshwater carbonates can be found. The colours of the limestone beads vary from white to red to grey or brown. All beads which could not be classified as “greenstone” or limestone were assigned to a third group, named “diverse beads”. Those beads vary considerably in their optical and chemical properties.

## Results and Discussion

### “Greenstone” Beads

The 17 “greenstone” beads that were analysed in the present study are listed in Table 1 and Table 2. Due to their greenish to turquoise colour, their copper-content, and specific texture, two different copper-minerals could be substantiated: the minerals turquoise and chrysocolla. As mentioned above, amazonite was grouped within this sub-category due to its colour, even though it contains copper only as a trace element.

Ornaments made of turquoise have been discovered at Prehistoric sites in the Near East from the Epipaleolithic onwards (Goring-Morris 1991: Fig. 19; Bar-Yosef Mayer and Porat 2008). A chronological evaluation of Maier’s (2008) analyses of “greenstones” from Beidha shows that turquoise increased during the Middle Pre-Pottery Neolithic B compared to the Natufian occupation phase. Similar observations were made by Alarashi (2014: 182-183) for the Late PPNB phase of Halula on the middle Euphrates, where the number of turquoise beads rose from 10% (n=25) during the Middle PPNB to 17% (n=150) in the Late PPNB. The name turquoise

originates from the French word “Turquie”, because material from Iranian sources was imported through Turkey (Anthony *et al.* 2000-2003). Its natural colour varies between sky blue, teal, and green. Characteristic for turquoise are brown, grey to black veins of other minerals. The density of turquoise varies with the porosity of the mineral. Typically, a density of 2.86g/cm<sup>3</sup> should be measured (Anthony *et al.* 2000-2003), although the density can be higher if the material is more compact. For usage as gemstones, the specimens with little to almost no veins are the most sought-after. In terms of abundance turquoise is a rare mineral. It is formed through weathering at the surface of hydrothermal copper deposits. It is a water-bearing Copper-Aluminium-Phosphate and its ideal molecular formula is:  $\text{CuAl}_6(\text{PO}_4)_4(\text{OH})_8 \cdot 4\text{H}_2\text{O}$ .

The mineral chrysocolla occurs in shades of greenish to turquoise colour and, as the mineral is relatively easy to work and shape, it has also been popular as a gemstone since Prehistoric times (*e.g.*, Hauptmann 2004; Maier 2008; Benz *et al.* 2020). The measured density of chrysocolla varies between 1.93 and 2.40g/cm<sup>3</sup> (Anthony *et al.* 2000-2003) and is lower than the density of turquoise. In contrast to turquoise, chrysocolla belongs to the group of silicates. The ideal molecular formula is:  $(\text{CuAl})_2\text{H}_2\text{Si}_2\text{O}_5(\text{OH}_4) \cdot n\text{H}_2\text{O}$ .

In nature, intergrowth of both minerals is very common, and an exact visual/ macroscopic determination is often impossible. Chemically both minerals contain copper (Cu), aluminium (Al), and water (H<sub>2</sub>O). Therefore, the elements that allow for a distinction, are phosphorus (P) in the structure of the turquoise and silicon (Si) in the structure of chrysocolla.

Amazonite is the green variation of microcline, therefore being a member of the feldspar group. Its main chemical composition is  $\text{K}(\text{AlSi}_3\text{O}_8)$ . The origin of its green colour is a matter for debate – possibly it results from traces of copper (Hauptmann 2004: 174). Amazonite has been used for ornaments at the latest since Neolithic times (Hauptmann 2004; Bar-Yosef Mayer and Porat 2008; Maier 2008; Gubenko and Ronen 2014). Workshops of amazonite bead production, dating to the Pre-Pottery Neolithic B,

were uncovered in southwestern Jordan, at Jebel Rabigh, Jebel Arqa, and Jebel Salaqa in the Hisma Basin (Vanucci *et al.* 1991; Balzi *et al.* 1998; Fabiano *et al.* 2004).

### ***Chemical Composition and Nomenclature of “Greenstone” Beads***

The chemical composition of the beads was determined using XRF. While these results can only be considered to be semi-quantitative, they are highly compliant with the theoretical composition of the respective minerals. The results are given in (Table 1 and Table 2). Following geochemical conventions, contents of main elements except Cu are shown as oxides. Our analyses show that chrysocolla and turquoise beads mainly consist of: Si, Al, Fe, Mg, Ca, Na, K, P, S, and Cu. Wide variations in values can be observed, for example for SiO<sub>2</sub> which ranges from 11.57wt.% to 36.08wt.%, Al<sub>2</sub>O<sub>3</sub> from 3.82wt.% to 41.60wt.%, P<sub>2</sub>O<sub>5</sub> from 1.00wt.% to 29.54wt.%, and Cu from 7.45wt.% to 58.58wt.%. All other main elements besides Si, Al, P, and Cu are supposed to have their origin in the intergrowth of additional minerals. Remarkable is Bead F.no. 100814.W Box 3 ECXXX because of its high Fe<sub>2</sub>O<sub>3</sub> value based on red-brown intergrowth of iron-minerals.

Fig. 1 shows a graphical overview of the chemical composition of seven beads identified as turquoise beads. In a first step, the values of the main components were normalised to 100% in order to adjust values from different scales so that the components can be compared directly. For visualisation each component has been given a different colour. The colours belonging to a sample were arranged in a bar. The last bar in the diagram shows an ideal composition for turquoise. Except for Bead F.no. 100814.W Box 3 ECXXX, all beads have Al, P, and Cu as dominant components. Some beads show noticeable values of Si, Fe, and Ca which can be explained by further constituent minerals (brown spots and veins within the bead).

In Fig. 2 the graphical synthesis of the chemical composition of nine beads which were identified as chrysocolla beads are shown, and one bead (F.no. 30800) identified as amazonite. The main components are also

normalised to 100% and the last bar of the chrysocolla group in the diagram represents an ideal chemical composition of chrysocolla for better comparison. The dominant components of the chrysocolla beads are Si and Cu. Almost all beads show a good match of their respective composition with the “ideal” chrysocolla. The Beads F.nos. 110825.916, 110825.788A, and 110825.788C show a relatively wide variation of major constituents. This could be due to more unfavourable measurement conditions, as they were already broken into pieces.

The Bead F.no. 30800 has a light green colour. Its main elements are Si, Al, and K. This chemical signature matches well the supposed mineral microcline K(AlSi<sub>3</sub>O<sub>8</sub>) – more precisely named amazonite. In Fig. 2 the eleventh and twelfth bar show the actual chemical composition of Bead F.no 30800 and the ideal composition of microcline.

### ***Trace Elements of “Greenstone” Beads: Evidence of Origin***

While using the main components for the identification of the mineral type of “greenstone” beads, the observed trace elements could provide evidence as to the origin of the beads. In Figs. 3 and 4 all analysed elements of turquoise and chrysocolla beads, except for the main components, were normalised to 100% and graphically ordered as bar graphs. Certain “colour patterns” can be observed and groups can be generated. The clusters are based on the concept, that every mineral deposit, where the minerals detected in the beads might come from, has its own individual conditions of genesis, geological setting, and possible alterations as weathering or metamorphosis. This results in an individual paragenesis of minerals and elements that can be regarded as a fingerprint of a mineral deposit.

In Fig. 3 the normalised trace elements of turquoise beads are shown graphically, and it seemed feasible to assign the beads to four patterns or groups. The determinant components of the first group are: Cl, Cr, Mn, Ni, Sr, and Zn. The Beads F.nos. 100814.117 and 100814.Zb belong to this group. Both beads were part of the necklace of the child

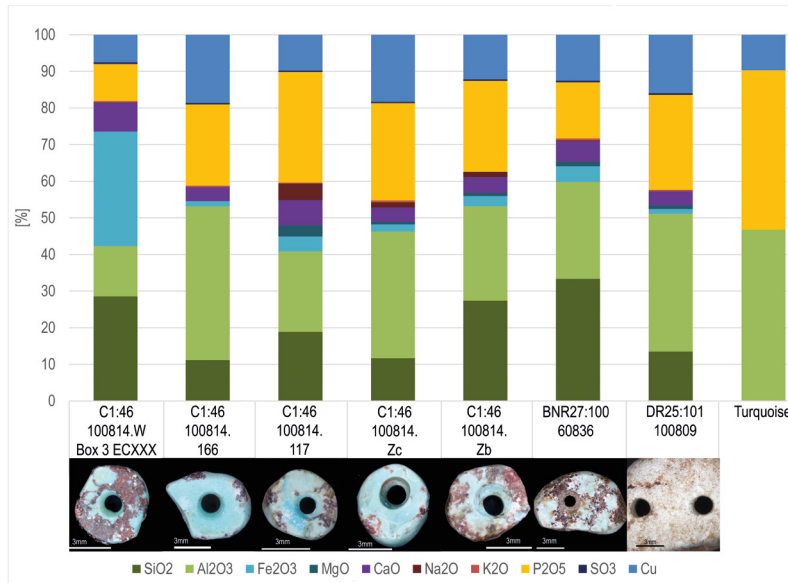


Fig. 1 Main elements of turquoise beads. (Graph: M. Gerlitzki, Ba`ja N.P.)

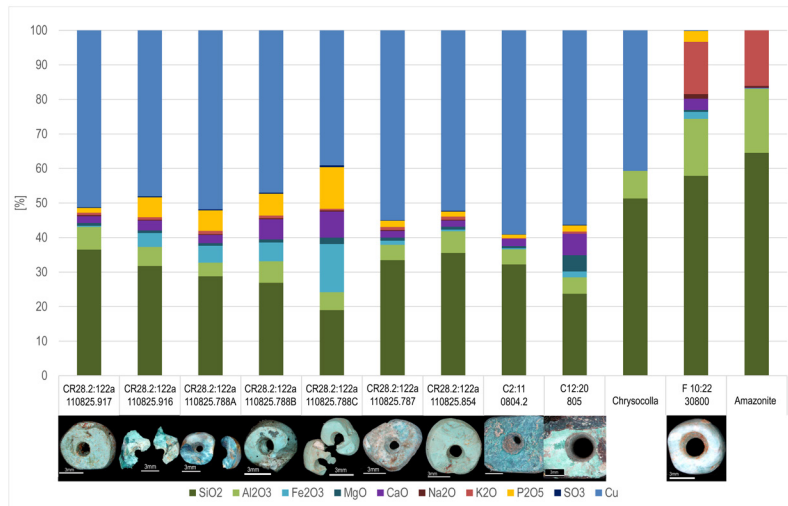


Fig. 2 Main elements of chrysocolla and amazonite beads. (Graph: M. Gerlitzki, Ba`ja N.P.)

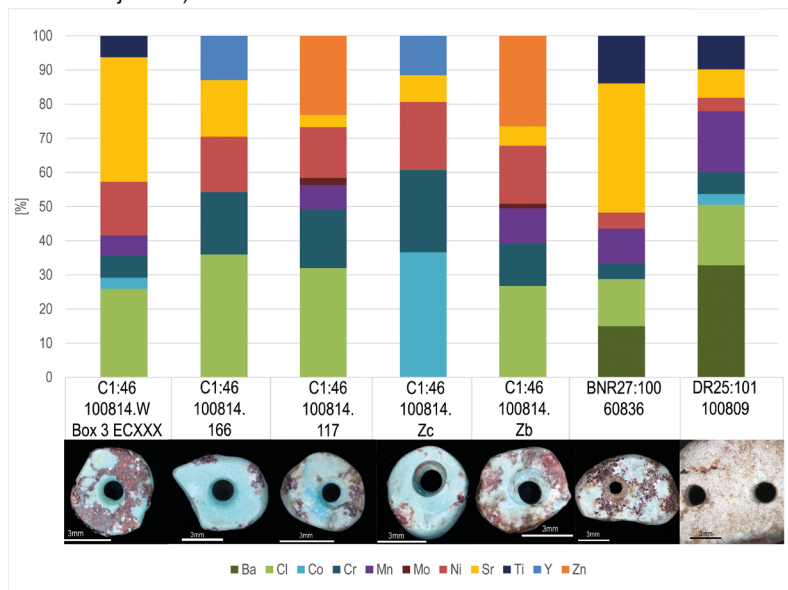


Fig. 3 Trace elements of turquoise beads. (Graph: M. Gerlitzki, Ba`ja N.P.)

Grave CG7, Loc. C1:46 (“Jamila”; see Alarashi b this volume; al-Sababha and Serbil this volume; Benz *et al.* this volume; Costes and Fischer this volume). In the second group that comprises beads of the same jewellery, the components Cl, Cr, Ni, and Sr are the dominant trace elements. The Beads F.nos. 100814.W Box 3 ECXXX and 100814.166 belong to this 2<sup>nd</sup> group. While Bead F.no. 100814.W Box 3 ECXXX additionally contains Co, Mn, and Ti, Bead F.no. 100814.166 has Y as additional trace element. An exception from the aforementioned Loc. C1:46 is Bead F.no. 100814.Zc, which has a high Co value beside the Cr, Ni, Sr, and Y values. It belongs to group three. The fourth group, Beads F.nos. 60836 and 100809, shows as dominant elements Ba, Cl, Cr, Mn, Ni, Sr, and Ti. At least three different sources of the turquoise minerals can thus be suggested. Whereas the almost perfect accordance of trace elements of the Beads F.nos. 100814.117 and 100814.Zb supports the thesis of a common mineral source, the beads F.nos. 100814.W Box 3 ECXXX and 100814.166 also show (disregarding Zn) substantial similarity. Therefore, one common source for Group 1 and Group 2 can be considered. Although the Beads F.nos. 60836 and 100809 have different optical properties and are from different loci (BNR27:100 and DR25:101), they show a very similar trace element pattern. This could be evidence of a common mineral origin, which is obviously different to that of Group 1 and Group 2. The high Co content of Bead F.no. 100814.Zc argues maybe for a fourth mineral source.

Identifying the sources of mineral artefacts such as beads, by comparison with ore samples, is problematic for several reasons, not least being that for bead production, presumably raw materials were chosen that were optically as pure as possible. Moreover, measurements of the prehistoric beads could only be carried out on the surface. A systematic analysis of the origin of the various minerals that were identified for Ba`ja (turquoise, chrysocolla, and amazonite) is therefore still pending.

The copper deposits on the Sinai Peninsula can be considered as nearest source of turquoises (Hauptmann 2020). For

the turquoises, a few observations for the analysed beads are listed here. The high nickel component of groups 1/ 2-3 (>0.128-0.319) is striking. Only F.nos. 60836 and 100809 show percentages below 0.06. Not one of the ores from Sinai analysed by Pfeiffer (2013: 114, Table 12) has values nearly as high as Group 1/ 2-3. Only three samples from unspecified sites in North Sinai and from Sheik Muhsen, a site near the copper deposits of Wadi Riqueita/ Wadi Rimthi in central southern Sinai, have values between 0.056 and 0.076. Both Beads, F.nos. 60836 and 100809, differ not only in their nickel content, but attest also strikingly to high barium values, for which no comparisons are available.

Relatively high zinc values, akin to Beads F.nos. 100814.117 and 100814.Zb, are found in the ore samples measured by Pfeiffer in the turquoises of Serabît el-Khadim, as well as in ores from Umm Bogma, Wadi Tar, and Wadi Rimthi. However, no turquoise deposits are mentioned in the latter three sources (Pfeiffer 2013: 33-34). Both beads with the high zinc values also have relatively high nickel values, 0.265% and 0.319%, which distinguish them from all four deposits of the Sinai mentioned (<0.001%-0.022%). The high cobalt value of Bead F.no. 100814.Zc is also unusual. It has not been measured in any sample from Pfeiffer. In regard to strontium values, three beads have rather high values between 0.131-0.429, which might be promising for an isotope analyses to identify their provenance.

It also seems worth mentioning that only the turquoise Button F.no. 100809 shows a strong bleaching of the colour, as is typical for turquoises from Serabît el-Khadim (Hauptmann 2004: 173). Such a strong bleaching was also observed for a very similar turquoise button (F.no. 110815) found in the child Grave DG2 (Loc. DR19:101), which was identified as turquoise in comparison with F.no. 100809. Bleaching has also been observed for some beads from the Graves CG5 (Loc. CR6:23a) and CG10 (Loc. C10:408) (*cf.* Benz *et al.* this volume), all of which, however, have not been analysed so far. Similar observations of bleaching were already made by A. Hauptmann (2004) for the turquoise beads from Basta.

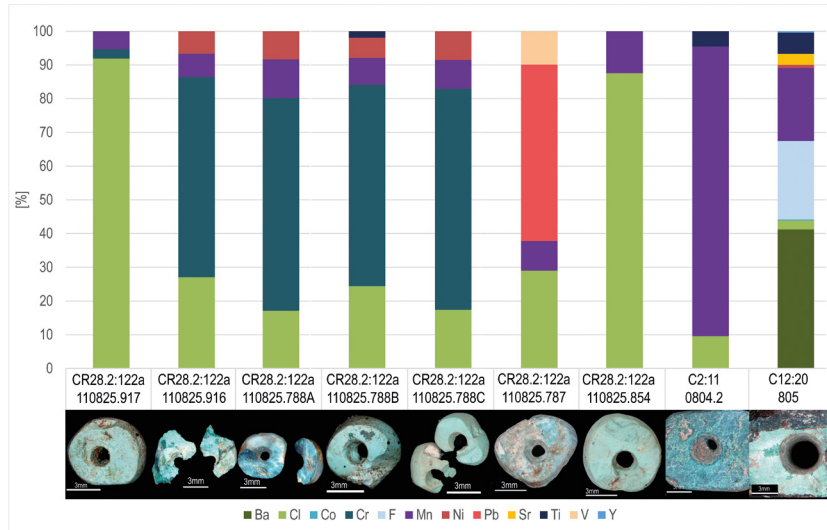


Fig. 4 Trace elements of chrysocolla and amazonite. (Graph: M. Gerlitzki, Ba`ja N.P.)

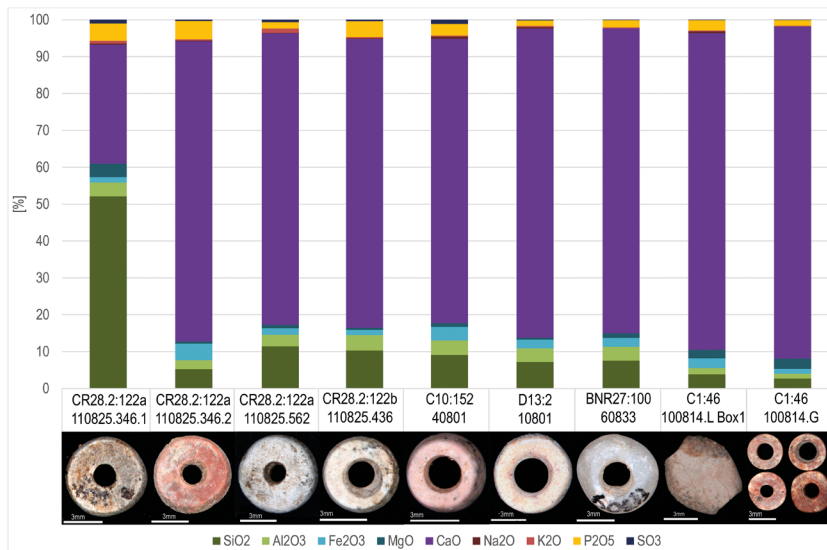


Fig. 5 Main elements of limestone beads. (Graph: M. Gerlitzki, Ba`ja N.P.)

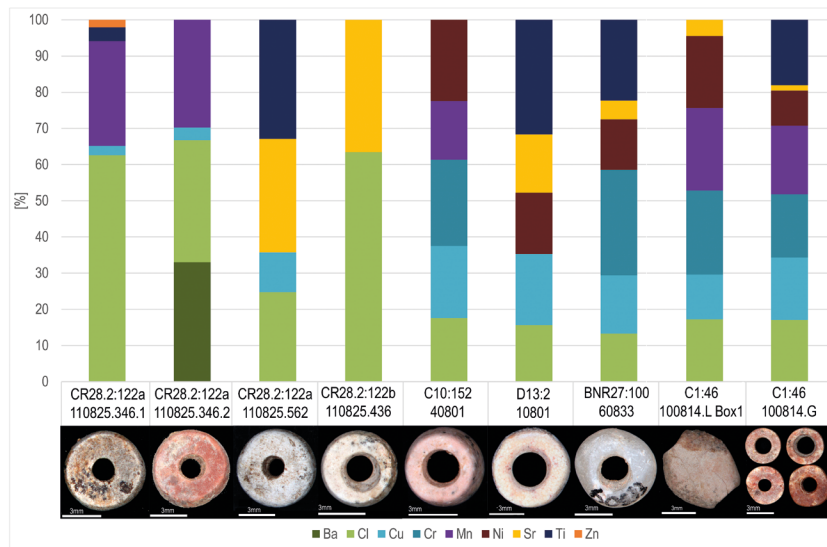


Fig. 6 Trace elements of limestone beads. (Graph: M. Gerlitzki, Ba`ja N.P.)

To conclude, the two turquoise Beads F.nos. 60836 and 100809 differ fundamentally from the other turquoise beads in regard to their trace elements. However, none of the beads seem to correspond to the turquoises from Serabît el-Khadim due to their high nickel content. The Button F.no. 100809 is the closest, with a nickel value of 0.016, which, however, exceeds the values of Serabît el-Khadim by a factor of 10. Likewise, none of the ore samples had a cobalt value nearly as high as that of Bead F.no. 100814.Zc. As potential sources three other small occurrences of turquoise east of the Red Sea, at Ziba, Aynuneh, and Gebel Shekayk could perhaps be taken into consideration (Hauptmann 2004: 173).

In Fig. 4 the normalised trace elements of chrysocolla beads are shown as colour bars, and it is evident that six out of nine beads can be grouped in one or two “colour patterns” (Group 1-2), while the remaining three beads are individual in their trace element composition. The dominant trace elements of Beads F.nos. 110825.917 and 110825.854, both from the jewellery of one of the older children (Loc. CR28.2:122a) within the multiple child Grave CG9, are Cl and Mn. From the same jewellery but in a possible second group, are the Beads F.nos. 110825.916, 110825.788A, 110825.788B, and 110825.788C. They have Cl, Cr, Mn, and Ni as dominant trace elements. Be it one or two groups, all samples could come from the same source. Bead F.no. 110825787 which was also part of the same jewellery of Loc. CR28.2:122a is an exception with regards to its trace element composition (Cl, Mn, Pb, and V). It also has a high amount of intergrowth of other minerals. The two bigger chrysocolla Beads F.nos. 0804.2 and 0805 have very different optical properties, as well as different trace element patterns. Bead F.no. 0804.2 found at Loc. C2:11 has the dominant trace elements Ce, Cl, Mn, and Ti, and Bead F.no. 0805 found in Loc. C12:20 has the dominant trace elements Ba, F, Mn, and Ti. Taken together, the last three beads might originate from three different sources, while the almost perfect accordance of trace elements of the Beads F.nos. 110825.916, 110825.788A, 110825.788B, and 110825.788C argues for a common ore genesis. The Beads F.nos. 110825.917 and 110825.854 could however also stem from this same deposit.

Timna and Faynan are well-known as sources of copper ores. The typical mineral paragenesis at both localities is chrysocolla, (par)atacamite, malachite, and diopside (Hauptmann 2020). The minerals atacamite and paratacamite consist partially of chlorine, so that the distinct content of Cl in the beads found at locus CR28.2:122a could hint at Timna/ Faynan as possible sources. Because the Beads F.nos. 0804.2 and 0805 show a different chemistry, we would suggest that they might come from different sources.

The copper content of almost all chrysocolla beads matches quite well with the contents observed for the copper ores at Wadi Faynan (Hauptmann 2007: 71). The rather high iron content of beads of “Group 2” might speak in favour of Timna as a source. However, their high manganese values do not match with the trace element signature from Timna, while the silt- and mudstones of the Faynan Dolomite-Limestone-Shale (DLS) comprise manganese ores (Hauptmann 2007: 73). The lowest percentages of manganese occur in beads of Group 1 (F.nos. 110825.917 and 100825.854), with 0.065% and 0.099 %, akin to manganese contents recorded from the Timna Formation (0.05%). To test the hypothesis of Timna as a possible origin, cuprified plant remains might give more evidence, because they are absent in the copper ores from Faynan (Hauptmann 2007: 72 *e.g.*, a mineral sample [F.no. 27887] from the Late PPNB site of Basta shows such cuprified plant remains, see Hauptmann 2004: 173). However, until yet, no mining traces have been found at Timna, dating before the Chalcolithic Period (pers. comm. D. Bar-Yosef Mayer).

Rather high nickel values of Group 2 beads point to the provenance from the Wadi Araba Region, but it is impossible to differentiate between Timna and Faynan by this trace element. The cobalt content for all chrysocolla beads is conspicuously low. Such low values have only been observed for ores that also have very low manganese and low nickel values (*cf.* Hauptmann 2007: Table A.1a).

To conclude, the chemical analyses show that chrysocolla beads were not from one, but at least two or possibly three sources (according to their differences in trace elements)

with Timna and Faynan both being possible sources. Similar observations have been made for the Middle PPNB site of Beidha, where Maier found evidence for Wadi Faynan and Timna as being possible sources for malachite (Maier 2008: 34)

Interestingly, beads of Group 1 and 2, which are rather similar in composition, belong to one ornament. F.no. 110825.787 is considerably different, but comes from the same jewellery. Beads F.nos. 0804.2 and 0805 are from more recent phases of occupation in the settlement, and were found in the deposit of an ancient oven as well as in floor debris.

Analyses of amazonite from Jebel Rabigh (Vanucci *et al.* 1991) show a rather similar composition, as the amazonite Bead F.no. 30800 from Ba`ja, comprising trace elements Fe, Ti, Mg, Cr, and Ni (except for Mn which could not be detected in that bead). Unfortunately, Vanucci *et al.* do not list the amount of trace elements, but their presence or absence, which hampers a more precise comparison. The Na<sub>2</sub>O (1.32%) contents of the bead from Ba`ja is slightly higher compared to amazonite from Jebel Rabigh (0.36%), but that may be due to the bead's surface measurements. Balzi *et al.* (1998: 363) have suggested that the amount of albite inclusions correlate with the content of Na<sub>2</sub>O, and can be used to differentiate amazonite from different sources. According to lead isotope similarities, they surmised in their analyses the pegmatitic rocks near Tabuk/Tbeik, in northwestern Saudi Arabia. However, as nearer potential sources for amazonite, the pegmatitic rocks of the Precambrian basement of Wadi Araba (Wadi Barqa) or in the region 30-40km southeast of Basta, should also be considered (Hauptmann 2004: 174).

### **Limestone Beads**

The chemical results from the limestone beads analysed in the present study are listed in Table 3. Based on their chemistry, their white, grey or red colour and their macro- and microscopic appearance, these beads could be identified as limestone.

In general, limestones can be differentiated due to their textural attributes, or due to their formation history. In this study the limestone beads were classified into four groups: biogenic limestone, chemical (abiogenic) limestone, clastic limestone, and crystalline limestone. Limestone with biogenic origin are the most abundant depositions of microorganisms, such as algae, foraminifers or molluscs. Chemical limestone is formed by the direct precipitation of calcium carbonate from marine or fresh water. Clastic limestone is formed by the cementation of calcitic sand and/ or mud. Crystalline limestone, such as marble, is a metamorphic rock composed of recrystallised carbonate minerals like calcite and dolomite. They are formed under high pressure and/ or temperature conditions, for example during orogeny.

In the limestone groups described here, the carbonate minerals are the essential minerals. The most frequently found carbonates are the chemical compounds of carbon (C), oxygen (O), and calcium (Ca), magnesium (Mg) or iron (Fe). The mineral calcite, calcium carbonate CaCO<sub>3</sub>, is among the most abundant minerals in the earth's crust, and it is the main component of limestone. Other important carbonate minerals are dolomite CaMg(CO<sub>3</sub>)<sub>2</sub> and magnesite MgCO<sub>3</sub>. The colour of limestone can vary from white (pure calcium carbonate) to red (Fe as colouring component) or to grey and black (colour due to organic matter).

### **Chemical Composition and Nomenclature of Limestone Beads**

In Fig. 5 the main components SiO<sub>2</sub>, Al<sub>2</sub>O<sub>3</sub>, Fe<sub>2</sub>O<sub>3</sub>, MgO, CaO, Na<sub>2</sub>O, K<sub>2</sub>O, P<sub>2</sub>O<sub>5</sub>, and SO<sub>3</sub> are shown in different colours. With the exception of the first bead, the colour bars show, at a first glance, that all remaining beads share almost the same chemical composition. The chemical composition in detail is shown in Table 3. The CaO values vary between 75.5wt.% and 89.5wt.%, SiO<sub>2</sub> between 2.6wt.% and 11.3wt.%, Al<sub>2</sub>O<sub>3</sub> between 1.2wt.% and 4.1wt.% and Fe<sub>2</sub>O<sub>3</sub> between 1.3wt.% and 4.4wt.%. In contrast, the first Bead F.no. 110825.346.1 has 31.9wt.% CaO, 51.5wt.% SiO<sub>2</sub>, 3.7wt.% Al<sub>2</sub>O<sub>3</sub>, and 1.5wt.% Fe<sub>2</sub>O<sub>3</sub>. According to this

Table 3 Chemical composition of limestone beads. Non-det.=not analysed, fields without numbers had a content below <0.005%.

Object	110825.346.1	110825.346.2	110825.562	110825.436	40801	10801	60833	100814.L Box1	100814.G
Locus	CR28.2:122a	CR28.2:122a	CR28.2:122a	CR28.2:122b	C10:152	D13:2	BNR27:100	C1:46	C1:46
SiO <sub>2</sub> [%]	51.56	5.21	11.33	10.30	8.91	7.13	7.47	3.79	2.69
Al <sub>2</sub> O <sub>3</sub> [%]	3.71	2.41	3.14	4.13	3.87	3.71	3.73	1.69	1.28
Fe <sub>2</sub> O <sub>3</sub> [%]	1.50	4.46	1.77	1.44	3.59	2.36	2.40	2.68	1.35
MgO [%]	3.59	0.541	0.882	0.537	0.973	0.520	1.26	2.24	2.76
CaO [%]	31.95	80.76	78.45	78.12	75.51	83.21	82.00	85.24	89.57
Na <sub>2</sub> O [%]	0.288	0.173	0.073	0.174	0.473	0.363		0.454	
K <sub>2</sub> O [%]	0.735	0.367	1.16	0.298	0.334	0.327	0.291	0.259	0.205
P <sub>2</sub> O <sub>5</sub> [%]	4.63	4.90	1.69	4.32	3.04	1.49	1.91	2.75	1.55
SO <sub>3</sub> [%]	1.01	0.323	0.665	0.377	1.11	0.159	0.095	0.109	0.056
Ba [%]		0.275							
Cl [%]	0.649	0.281	0.182	0.198	0.208	0.115	0.112	0.124	0.090
Cu [%]	0.027	0.029	0.081		0.237	0.145	0.135	0.089	0.091
Cr [%]					0.282		0.245	0.167	0.092
Mn [%]	0.300	0.248			0.192			0.164	0.100
Ni [%]					0.266	0.125	0.117	0.143	0.051
Sr [%]			0.231	0.114		0.119	0.044	0.032	0.008
Ti [%]	0.040		0.242			0.233	0.187		0.095
Zn [%]	0.021								
<b>Total</b>	<b>100.0</b>	<b>100.0</b>	<b>99.9</b>	<b>100.0</b>	<b>99.0</b>	<b>100.0</b>	<b>100.0</b>	<b>99.9</b>	<b>100.0</b>
Density [g/cm <sup>3</sup> ]	non-det.	non-det.	non-det.	non-det.	2.60	2.53	2.74	2.59	2.72
Colour Texture	light grey, very small components, angular quartz grains	red color due to Fe, micrite	light grey, micrite	white, laminated, porose, very small quartz grains	white to light red	white	white, compact	red, clastic texture	red, micrite
Supposed material	clastic limestone	chemical limestone	chemical limestone	biogene limestone	biogene limestone (coral?)	biogene limestone (coral?)	crystalline limestone (marble?)	clastic limestone	chemical limestone

analysis and the microscopical observations, the bead contains additional minerals besides calcite. The high percentage of SiO<sub>2</sub> reveals quartz, and the Al<sub>2</sub>O<sub>3</sub> value corresponds to a small amount of clay minerals. This bead exhibits also macroscopically, visible grains, and can therefore be described as clastic limestone. Due to their chemical composition, colour, and micritic texture (no visible grains), Beads F.nos. 110825.346.2, 110825.562, and 100814.G can be identified as chemical limestone beads. Bead F.no. 100814.L Box 1 shows a clastic texture, and the particles are

macroscopically visible, therefore it is also named a clastic limestone. In contrast, Bead F.no. 60833 has a crystalline texture and a compact appearance indicating that it is marble. Beads F.nos. 40801 and 10801 (due to their texture) addressed as biogenetic carbonates, may be identified as coral beads. Bead F.no. 110825.436 has a laminated porous texture and very small quartz grains. Microscopically the pores are reminiscent of holes created by incrustation of microorganisms. Therefore, this last-mentioned bead also belongs to the group of biogenetic limestone.

Table 4 Comparison of Dabba Marbles (median) elements and results of Bead F.no. 60833 from Ba'ja. Raw material samples for Wadi Jilat were taken 15km to the west of Wadi Jilat 13 by A. Garrard; for the Dabba Marbles the max. ranges are indicated after (Wright *et al.* 2008: Tables 8 and 9); all measurements are given in %, except for trace elements which Wright *et al.* recorded in ppm, only their relative amount is indicated: +++ high, ++ medium, + low.

F.no.	Prove-nance	SiO <sub>2</sub>	Al <sub>2</sub> O <sub>3</sub>	Fe <sub>2</sub> O <sub>3</sub>	MgO	CaO	Na <sub>2</sub> O	K <sub>2</sub> O	P <sub>2</sub> O <sub>5</sub>	SO <sub>3</sub>	Ba	Cl	Cu	Cr	Mn	Ni	Sr	Ti	Zn
G1-2	Dabba	1.8-	0.00-	0.14-	0.00-	48.5-	0.1-		3.99-			0.00-			0.00-			0.049-	
LG1-3	Marbles	7.6	1.7	1.72	2.50	57.7	0.9	0.00	13.03	0.00	+/++	0.4	+	++	0.024	+	+++	0.134	+++
R1	(min-max)																		
(n=6)	Median	5.20	0.90	1.01	0.25	53.45	0.45	0.00	7.84	0.00		0.00			0.01			0.07	
60833	Ba'ja BNR27:100	7.47	3.73	2.4	1.26	82	0	0.291	1.91	0.095	0	0.112	0.135	0.245	0	0.117	0.044	0.187	0

### **Trace Elements of Limestone Beads: Evidence of Origin?**

A visual compilation of analysed trace elements from the limestone beads is shown in Fig. 6. As before, all trace elements were normalised to 100%. The Beads F.nos. 110825.562, 110825.436, and 10801 have remarkably high Sr values. Beads F.nos. 110825.346.1, 110825.346.2, and 110825.436 have high values for Cl. Both elements, are so called tracer elements and can be a sign for enrichment in marine environment. These values indicate that isotope analyses seem to be promising for further provenance studies.

To track down the possible source of different limestones is rather difficult because many possible local sources have to be considered. The detailed study of genetic features, and the exact naming of the types of limestones and comparing items to regionally occurring limestones, might be worthwhile. It is very likely that the limestone beads come from a local or regional source, because limestone deposits are so abundant. In comparison to non-metamorphous limestone, marble is scarce. As one possible source for the marble Bead F.no. 60833, the Dabba Marble (Wright *et al.* 2008) can be taken into consideration. However as the median of the Dabba Marbles shows, there are considerable differences (Table 4).

### **Thin Sections of Disk Beads**

For a more detailed analysis of the texture of the carbonate Beads F.no. 100814.G also named disk beads, three of them were chosen for thin

section analysis, with the polarizing petrographic microscope. This method allows the identification of minerals based on their optical properties under polarised light. The most distinguishing optical properties are colour, refraction index, interference colour and cleavage property. Texture, grain size, and intergrowth of mineral grains as well as possible cavities can also be observed. In biogenic limestones microfossils can often be detected that also contribute to the diagnosis of a limestone and its specific formation process.

The picture on the left of Fig. 7 is an image of one of the three disk beads, chosen for the preparation of thin sections. Macroscopically they show a red colour, certainly due to the occurrence of hematite. The texture seems to be micritic. Fossils or other biogenetic textures are not visible so far. The diameter of the beads varies between 4 to 5mm.

The picture in the middle in Fig. 7 shows a cut-out of one thin section under plane-polarised light (PPL). The picture on the right shows the same cut-out under cross-polarised light (XPL). The beads are cut along their horizontal axis. The main mineral is calcite. Under PPL the calcite grains appear transparent colourless to brown, meaning that the grains are covered by a thin layer of hematite. The grain boundaries are very irregular and intertwined, which is typical for micritic carbonates. The transparent grains (PPL) show colours of high order (light blue-green-orange-pink) under XPL typical interference. The brown grains are also (under XPL) brown due to the hematite impregnation. No fossils or other

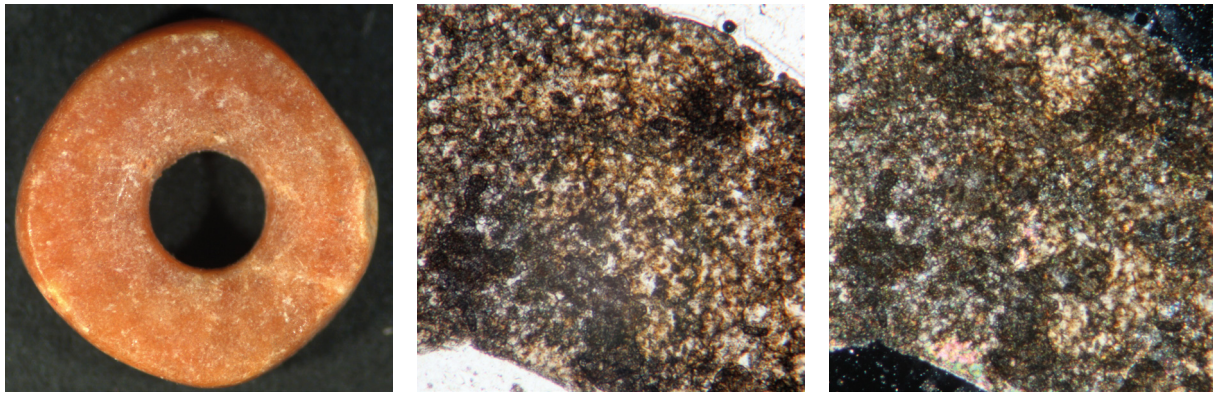


Fig. 7 Thin sections of disk beads. (Photos: M. Gerlitzki, Ba`ja N.P.)

Table 5 Chemical composition of „diverse“ beads. Non-det.=not analysed, fields without numbers had a content below <0.005%.

Objects	100814.E	100804	20830	110825.470	20833
<b>Locus</b>	C1:46	D32:399	DR26:26	CR28.2:122b	B74:16
<b>SiO<sub>2</sub> [%]</b>	3.40	89.40	0.951	31.13	6.69
<b>Al<sub>2</sub>O<sub>3</sub> [%]</b>	1.23	0.286	0.431	9.72	3.12
<b>Fe<sub>2</sub>O<sub>3</sub> [%]</b>	89.50	1.05	1.77	5.26	1.83
<b>MgO [%]</b>	0.559	0.821	0.166	0.984	0.751
<b>CaO [%]</b>	1.03	1.27	94.06	33.74	74.01
<b>Na<sub>2</sub>O [%]</b>	1.329	1.33	0.534	0.449	0.850
<b>K<sub>2</sub>O [%]</b>	0.098	0.116	0.046	1.70	0.557
<b>P<sub>2</sub>O<sub>5</sub> [%]</b>	1.81	2.69	1.23	9.35	1.53
<b>SO<sub>3</sub> [%]</b>	0.061	2.56	0.044	6.28	0.137
<b>Cl [%]</b>	0.255	0.247	0.089	0.694	0.089
<b>Cu [%]</b>	0.176	0.057	0.128		0.101
<b>Cr [%]</b>	0.037	0.105	0.149		0.104
<b>F [%]</b>					9.93
<b>Mn [%]</b>	0.203				
<b>Ni [%]</b>	0.225	0.075	0.155		0.084
<b>Sr [%]</b>			0.246	0.213	0.052
<b>Ti [%]</b>				0.493	0.162
<b>V [%]</b>	0.082				
<b>Total</b>	<b>100.0</b>	<b>100.0</b>	<b>100.0</b>	<b>100.0</b>	<b>100.0</b>
<b>Density [g/cm<sup>3</sup>]</b>	non-det.	2.60	2.86	non-det.	2.48
<b>Colour</b>	brown, compact, metallic luster	orange to red, slightly transparent		brown to grey, porous, laminated, dark components (ash?)	dark grey, micrite
<b>Texture</b>			laminated		
<b>Supposed material</b>	hematite	carnelian	aragonite (coral/shell?)	weathering product/volcanic?	limestone with high F?

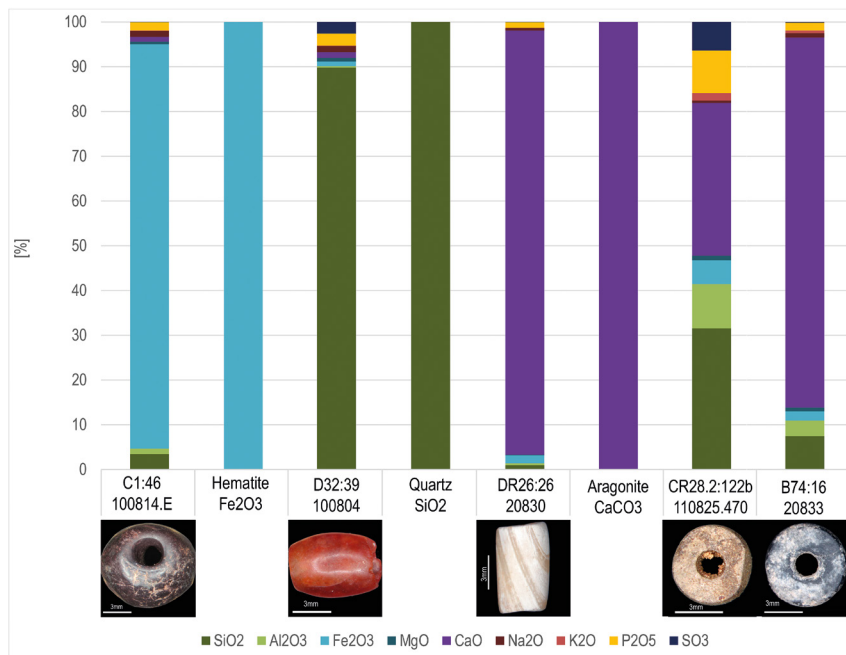


Fig. 8 Main elements of “diverse” beads. (Graph: M. Gerlitzki, Ba`ja N.P.)

textural characteristics are visible. Therefore the assumption of a chemical limestone with micritic texture is substantiated.

### ***Diverse Beads***

In addition to “greenstone” and limestone beads, five more beads were analysed that could not be assigned to either of the aforementioned groups. Macroscopically, they appear to be very individual, but typical for their respective minerals from which they are made. In Table 5, the chemical compositions of the beads are listed.

### ***Classification of the Diverse Beads and Possible Sources***

Compared to most other beads, the dark brown Bead F.no. 100814.E is relatively compact indicating a higher density. It has a metallic lustre, and the fissures appear red. The supposed mineral hematite,  $\text{Fe}_2\text{O}_3$ , is the main modification of iron(II)-oxide on earth. The measured density is about  $5.26\text{g/cm}^3$  (Anthony *et al.* 2000-2003) the typical colour is black to brown, and the colour of the weathered mineral is red. The first two bars of Fig. 8 show the chemical composition of Bead F.no. 100814.E as analysed, and the ideal

chemical composition of the mineral hematite. It is evident that its optical properties and the “colour patterns” of chemistry match very well. The bead can therefore be identified as a hematite bead. Hematite can be found in sedimentary, magmatic, and metamorphous environments, as well as in veins. That is why it is occurring so frequently. Hematite beads of an irregular, more or less spherical shape have been reported from Basta (Hermansen 2004: Fig. 2.2, 2.9) and pieces of hematite minerals were uncovered at Beidha (Maier 2008) and Ba`ja, too.

The Bead F.no. 100804 of an orange to red colour, is slightly transparent and relatively hard. The supposed material carnelian, is a non-transparent to slightly transparent orange to red variation of chalcedony. Chalcedony is a fibrous, microcrystalline variation of the mineral quartz ( $\text{SiO}_2$ ). In Fig. 8 the third and fourth bar shows the analysis of the bead, and for comparison the ideal chemical composition of quartz. The chemistry of both matches very well, and the bead can be clearly identified as carnelian. A source of carnelian is not known yet, even though carnelian was intensively worked in later times at the Northwest Arabian Oasis of Tayma (Purschwitz 2017).

Bead F.no. 20830 has an elongated shape and a distinctively layered texture. The colours of the layers alternate between white and light rose. This texture resembles the structure of a shell. The main component of the bead is  $\text{CaCO}_3$ . Shells often consist of the mineral aragonite. Aragonite is chemically the same as calcite –  $\text{CaCO}_3$  – but is predominantly formed by biological processes in freshwater or marine environments. The main difference between calcite and aragonite is the crystal system, thus resulting in different physical properties. For calcite, a density of  $2.71\text{g/cm}^3$  (Anthony *et al.* 2000-2003) is typical. The density of aragonite is about  $2.95\text{g/cm}^3$ . The exact density of Bead F.no. 20830 is  $2.86\text{g/cm}^3$ , which gives additional evidence for aragonite as a mineral, and a shell as raw material. Protein analyses on a similar bead identified the raw material as *Tridacna* sp. (Alarashi in this volume, *cf.* Hermansen n.d.; see also Nissen *et al.* 1987: Fig. 18.27-28).

Bead F.no. 110825.470 has a brown to grey colour with a porous texture. The raw material seems to be clastic and some dark grains are visible (maybe ash?). The main components (see Fig. 8) are Si, Ca, Al, Fe, P, and S. These combinations of chemical components could be a product of weathering, but for a detailed identification further analyses are needed.

Bead F.no. 20833 has a dark grey to black colour. The appearance is compact, and the measured density is  $2.49\text{g/cm}^3$ . The main components are Ca, Si, and F. Raw material with such high F values are special in geoscience, but to confirm those values and for a detailed identification further analyses are again needed.

## Conclusion

A total of 31 beads was analysed in this study. They were made from a variety of geological materials. Tables 1 to 3, and 5 show their mineralogical and chemical composition. From the 17 “greenstone” beads, seven were identified as turquoise, nine as chrysocolla, and one as amazonite. In the limestone group two clastic limestones, three chemical limestones, three biogenic limestones and one crystalline limestone (marble) could be specified. In the diverse group one hematite bead, one carnelian, and one bead

made of a *Tridacna* sp. shell were identified. Two beads of the diverse group could not be identified in detail. While the chemical analyses were very helpful for the identification of the turquoise, chrysocolla, and diverse beads, for the limestone beads the textural microscopic analyses were especially helpful for classification.

For almost all of the (mineralogically very different) beads, several possible sources are mentioned in the literature. The wide variety of minerals confirm earlier observations, those of increased management of minerals for ornamentation with deliberate choices in procurement, production (with increasing sophistication in artificial shapes), and long object “biographies”, including recycling (*e.g.*, Bar-Yosef Mayer and Porat 2008; Wright *et al.* 2008; Alarashi 2016; Baysal 2017; Benz *et al.* 2019). The knowledge of different minerals must have been so specific, that the selection of minerals for jewellery was well planned and intentional. Our analyses suggest that in Burial CG7 (“Jamila”) only turquoises were used from the “greenstones”. In contrast, in the multiple subadult Burial CG9, according to the analysed beads obviously only chrysocolla was used from the “greenstones”, besides various shells and other stone beads. Neither malachite, nor turquoises nor amazonite were used in this burial, even though all these minerals have been documented at Ba`ja (Alarashi and Benz in this volume: Annex 1). Moreover, it has been shown that beads of the same mineral, albeit from several sources, were possibly combined in one jewellery.

The people from Ba`ja used raw materials from their surrounding area as well as raw materials from wider areas. We suppose that the limestone beads have their origin in the surrounding areas of Ba`ja, whereas the more colourful beads had their origin in wider areas.

The origin of the turquoise raw materials must be considered as unidentified so far. According to differences in trace elements, it seems rather unlikely that the turquoises – analysed to date – came from Serabit el-Khadim. However, this may be the case for the above-mentioned turquoise buttons: both are from more recent occupation phases, and are very heavily bleached, a characteristic of turquoises from Serabit el-Khadim. Furthermore, the

results of our analyses let us suggest, that the chrysocolla beads were most probably not from one source only. Differentiating between Wadi Faynan and the Timna Formation is very difficult, but high manganese values in most of the beads – with two exceptions – exclude Timna as a possible raw material source, and speak in favour of the DLS formations of the Wadi Faynan Area. Strikingly, copper mineral beads of younger phases of occupation seem to come from other sources than beads from the more ancient burials.

The supposed marble bead (F.no. 60833) does not match with the general composition of Dabba Marbles in central Jordan, which has been considered a source for marble beads from the PPNB sites of Basta (Hermansen

2004) and Beidha (Maier 2008). However, identifying sources of marble, especially on a very tiny bead, is fraught with many problems (e.g., Shqiarat *et al.* 2019). Therefore, our suggestions should be considered preliminary.

Future systematic trace element and isotope analyses of minerals and artefacts seem promising to provide valuable insights into the exchange networks, and their possible changes during the 7<sup>th</sup> millennium BCE.

**Melissa Gerlitzki and Manfred Martin**  
Landesamt für Geologie, Rohstoffe und  
Bergbau, Freiburg  
Melissa.Gerlitzki@rpf.bwl.de

## References

- Alarashi H.  
2014 *La parure épipaléolithique et néolithique de la Syrie (12e au 7e millénaire avant J.-C.): techniques et usages, échanges et identités*. PhD Thesis. Lyon: Université Lumière Lyon 2.
- 2016 The “butterfly” beads of the Levant: socio-cultural and economic implications during the Pre-Pottery-Neolithic B. *Cambridge Archaeological Journal* 26(3): 493-512.
- Anthony J.W., Bideaux R.A., Bladh K.W. and Nichols M.C. (eds.)  
2000-2003 *Handbook of Mineralogy*. Chantilly: Mineralogical Society of America.  
<http://www.handbookofmineralogy.org/>
- Balzi S., Sozzi M., Vannucci S. and Vaselli O.  
1998 A Pre-Pottery Neolithic stone: amazonite from southern Jordan sites. In: *XIII U.I.S.P.P. Congress Proceedings*, Forli, 8-14. Sept. 1996: 361-369. Forli: ABACO.
- Bar-Yosef D.  
1991 Changes in the selection of marine shells from the Natufian to the Neolithic. In: O. Bar-Yosef and F.R. Valla (eds.), *The Natufian culture in the Levant*. Archaeological Series 1: 629-636. Ann Arbor: International Monographs in Prehistory.
- Bar-Yosef Mayer D.E. and Porat N.  
2008 Green stone beads at the dawn of agriculture. *Proceedings of the National Academy of Sciences* 24(105): 8548-8551.
- Baysal E.  
2017 Personal ornaments in Neolithic Turkey, the current state of research and interpretation. *Journal of Archaeology and Art* 155: 1-22.
- Benz M., Gresky J. and Alarashi H.  
2020 Similar but different – displaying social roles of children in burials. In: Alarashi H. and Dessì R.M. (eds.), *The art of human appearance. 40<sup>e</sup> Rencontres internationales d'archéologie et d'histoire de Nice*: 93-107. Nice: APDCA.
- Benz M., Gresky J., Štefanisko D., Alarashi H., Knipper C., Purschwitz C., Bauer J. and Gebel H.G.K.  
2019 Burying power: new insights into incipient leadership in the late Pre-Pottery Neolithic from an outstanding burial at Ba`ja, southern Jordan. *PLoS ONE* 14(8):e0221171.  
doi:10.1371/journal.pone.0221171
- Clarke J.  
2012 Decorating the Neolithic: an evaluation of the use of plaster in the enhancement of daily life

- in the Middle Pre-Pottery Neolithic B of the Southern Levant. *Cambridge Archaeological Journal* 22(2): 177-186.
- Fabiano M., Berna F. and Borzatti von Löwenstern E.  
2004 Pre-Pottery Neolithic amazonite bead workshops in southern Jordan. In: Secretariat du Congrès (ed.), *The Neolithic in the Near East and Europe. Acts of the XIVth World Congress of the Union of Prehistoric and Protohistoric Sciences (UPPS)*, University of Liège (Belgium), 2-8 September 2001. BAR int. series 1303: 265-275. Oxford: Archaeopress.
- Gebel H.G.K., Benz M., Purschwitz C., Bader M., Dermech S., Graf J., Gresky J., Hájek F., Miškolciová L., al Khasawneh S., Khrisat B., Kubíková B., Renger M., al-Sababha M.H. and al-Shoubaki S.  
2020 Household and death, 3: preliminary results of the 13<sup>th</sup> season (spring 2019) at late PPNB Ba`ja, southern Jordan (interim report). *Neo-Lithics* 20, special issue (Ba`ja 2019 season, interim report): 3-41.
- Gebel H.G.K., Benz M., Purschwitz C., Kubíková B., Štefanisko D., al-Soulaiman A.S., Tucker K., Gresky J. and Abuhelaleh B.  
2017 Household and death. Preliminary results of the 11<sup>th</sup> season (2016) at late PPNB Ba`ja, southern Jordan. *Neo-Lithics* 1/17: 18-36.
- Goring-Morris N.  
1991 The Harifian of the Southern Levant. In: O. Bar-Yosef and F.R. Valla (eds.), *The Natufian culture in the Levant*. Archaeological Series 1: 173-216. Ann Arbor: International Monographs in Prehistory.
- Gubenko N. and Ronen A.  
2014 More from Yiftahel (PPNB), Israel. *Paléorient* 40(1): 149-158.
- Hauptmann A.  
2004 "Greenstones" from Basta. Their mineralogical composition and possible provenance. In: H.J. Nissen, M. Muheisen and H.G.K. Gebel (eds.), *Basta I. The human ecology*. bibliotheca neolithica Asiae meridionalis et occidentalis and Yarmouk University, Monograph of the Faculty of Archaeology and Anthropology 4: 169-176. Berlin: ex oriente.  
2007 *The archaeometallurgy of copper. Evidence from Faynan, Jordan*. Berlin: Springer.  
2020 *Archaeometallurgy – material science aspects*. Berlin: Springer International.
- Hermansen B.D.  
2004 Raw materials of the small finds industries. In: H.J. Nissen, M. Muheisen and H.G.K. Gebel (eds.), *Basta I. The human ecology*. bibliotheca neolithica Asiae meridionalis et occidentalis and Yarmouk University, Monograph of the Faculty of Archaeology and Anthropology 4: 117-128. Berlin: ex oriente.
- n.d. Beads from mineral, coral, and bone. In: B.D. Hermansen, H.G.K. Gebel and D.S. Reese (eds.), with a contribution by K. McNamara, *Basta IV.1. The small finds and ornament industries*. bibliotheca neolithica Asiae meridionalis et occidentalis. Berlin: ex oriente.
- Kodaş E.  
2019 A new aceramic Neolithic site in the Upper Tigris valley: preliminary results of Boncuklu Tarla. *Neo-Lithics* 19: 3-15.
- Maier R.  
2008 *Grünsteine und Grünsteinperlen aus Beidha. Jordanien*. M.A. Thesis. Bochum: Ruhr University.
- Maréchal C.  
1991 Eléments de parure de la fin du Natoufien: Mallaha Niveau I, Jayroud 1, Jayroud 3, Jayroud 9, Abu Hureyra et Mureybet IA. In: O. Bar-Yosef and F.R. Valla (eds.), *The Natufian culture in the Levant*. Archaeological Series 1: 589-612. Ann Arbor: International Monographs in Prehistory.
- Nissen H.J., Muheisen M. and Gebel H.G.  
1987 Report on the first two seasons of excavation at Basta (1986-1987). *Annals of the Department of Antiquities Jordan* 31: 79-119.
- Pfeiffer K.  
2013 *Neue Untersuchungen zur Archäometallurgie des Sinai. Die Entwicklungsgeschichte der Innovation „Kupfermetallurgie“*. Forschungs-Cluster 2. Innovationen: technisch, sozial. Menschen – Kulturen – Traditionen. Studien aus den Forschungslustern des Deutschen Archäologischen Instituts 11. Rahden: Leidorf.
- Purschwitz C.  
2017 The prehistory of Tayma. The chipped stone evidence. The surface finds and a technotypical analysis of the chert artefacts from the carnelian bead workshop SE 2. *Zeitschrift für Orient-Archäologie* 10: 288-311.
- Reese D.S.  
1991 Marine shells in the Levant: Upper Paleolithic, Epipaleolithic and Neolithic. In: O. Bar-Yosef and F.R. Valla (eds.), *The Natufian culture in the Levant*. Archaeological Series 1: 613-628. Ann Arbor: International Monographs in Prehistory.
- Santallier D., Maréchal C. and Véra R.  
1997 Éléments de parure du néolithique syrien. Identification et provenances des matériaux. *Revue d'Archéométrie* 21: 55-65.

Shqiarat M., Alnawafleh H. and Abudanah F.  
2019 Characterization and provenance study of marble  
from Udhruh, southern Jordan. *Mediterranean  
Archaeology and Archaeometry* 19(1): 1-8.

Vanucci S., Sozzi M., Vaselli O. and Vianello F.  
1991 Studio mineralogico e geochimico

dell'amazonite dell'atelier neolithico di Jebel  
Rabigh (Giordania). *Plinius* 6: 190-191.

Wright K.I., Critchley P. and Garrad A.  
2008 Stone bead technologies and early craft  
specialization: insights from two Neolithic sites  
in eastern Jordan. *Levant* 40: 131-165.